CHIN.PHYS.LETT. Vol. 25, No. 2 (2008) 608

Coupling of Evaporation and Thermocapillary Convection in a Liquid Layer with Mass and Heat Exchanging Interface *

JI Yan(纪岩), LIU Qiu-Sheng(刘秋生)**, LIU Rong(刘荣)
Institute of Mechanics, Chinese Academy of Sciences, Beijing 100080

(Received 17 October 2007)

We propose and analyse a new model of thermocapillary convection with evaporation in a cavity subjected to horizontal temperature gradient, rather than the previously studied model without evaporation. The pure liquid layer with a top free surface in contact with its own vapour is considered in microgravity condition. The computing programme developed for simulating this model integrates the two-dimensional, time-dependent Navier–Stokes equations and energy equation by a second-order accurate projection method. We focus on the coupling of evaporation and thermocapillary convection by investigating the influence of evaporation Biot number and Marangoni number on the interfacial mass and heat transfer. Three different regimes of the coupling mechanisms are found and explained from our numerical results.

PACS: 47. 27. Te, 68. 03. Fg, 02. 60. Cb

Investigations on mass and heat transfer at evaporating liquid–vapour interfaces are important because a number of applications, such as heat exchangers, distillation columns and combustion devises, are concerned about this phenomenon. Although it is adequate to assume in many applications that the liquid–vapour interface is nearly at complete equilibrium, namely the thermal and chemical potential equilibrium,[1] yet the non-equilibrium effect becomes especially important when a liquid is undergoing rapid evaporation at reduced pressure,[2,3] such as in heat pipes, where a great amount of energy is transported by the vapour to reach high heat exchanging efficiencies. In the microgravity environment, the thermocapilliarity mechanism is generally dominant, leading to thermocapillary convection, which may influence performances of the heat exchanger. It is therefore desirable to examine the role of thermocapillary convection on evaporation mass and heat transfer.

While many works have been performed to investigate evaporation phenomena, only a few papers addressed the Marangoni flow in evaporating liquids. Shih and Megaridis [4] presented an axisymmetric droplet model considering thermocapillary effect on the dynamic behaviour of a vaporizing–convecting droplet from a computational point of view. Savino and co-workers[5] carried out combined experimental and numerical analysis to study both steady and transient Marangoni effects in hanging evaporating droplets. Hu and Larson[6] studied the effects of Marangoni stress in an evaporating sessile droplet through analytical approach.

Although these scholars have developed theories for evaporating liquid with Marangoni effects, it should be noted that some important issues have still not been resolved: (i) Most models treat the gas phase as a mixture of the vapour and other gases, in which local thermodynamic equilibrium is assumed at the interface. In these models, evaporation flux lies on the mass diffusion induced by the gradient of vapour concentration in the gas, as well as the heat diffusion in the liquid layer. However, when the gas is exclusively composed by its pure vapour, the mass diffusion mechanism is eliminated. The non-equilibrium kinetics of evaporation reveals itself and competes with heat diffusion in dictating evaporation. This issue is raised in stability analysis,[1] but rarely studied by numerical simulation. (ii) Many researchers have focused on the evaporation of a liquid layer heated from bottom, with the surface-tension-driven instabilities induced by the vertical temperature gradient in the liquid. Nevertheless, the classical thermocapillary convection of an evaporating liquid layer subjected to horizontal temperature gradient has seldom been investigated. Motivated by the two points above, we devote to developing a model accounting for the interfacial mass and heat transfer with evaporation and thermocapilliarity.

The physical model consists of a rectangular cavity of height H and width D containing an incompressible, Newtonian liquid in contact with its own vapour. The left and right sides of the cavity are vertical rigid, isothermal walls. To maintain the upper free surface at a constant height, the bottom boundary is assumed to be an adiabatic porous medium though which liquid is injected to enable mass flow balance. This model is presented in Fig. 1.

We assume that the whole system (the liquid, the vapour, and the boundaries) first stays at saturation

*Supported by the National Natural Science Foundation of China under Grant Nos 10772185 and 10372105, and the Knowledge Innovation Programme of Chinese Academy of Sciences (KGCX-SW-409).
** To whom correspondence should be addressed. Email: liu@imech.ac.cn

temperature T_s at a certain vapour pressure. The thermodynamic equilibrium state is achieved with no convection. After a time, the temperature of the right wall suddenly increases to a higher value T_h. With horizontal temperature gradient in the liquid layer, thermocapillary convection is induced. As the surface temperature exceeds saturation temperature, net mass flux from liquid to its vapour is expected.

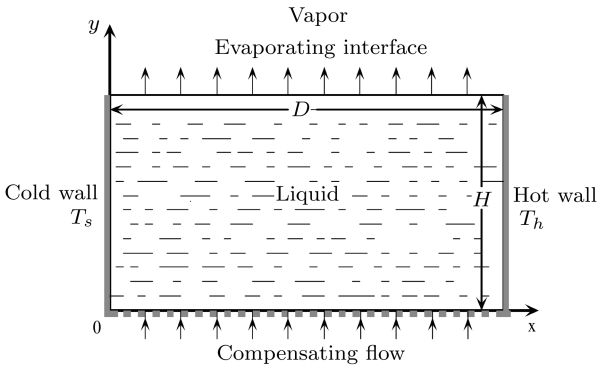

Fig. 1. Evaporation–thermocapillary model.

In the absence of gravity, the non-dimensional incompressible Navier–Stokes equations with Boussinesq approximation are

$$\nabla \cdot \boldsymbol{u} = 0, \tag{1}$$

$$\frac{\mathcal{D}\boldsymbol{u}}{\mathcal{D}t} = -\nabla p + \nabla^2 \boldsymbol{u}, \tag{2}$$

$$\frac{\mathcal{D}\theta}{\mathcal{D}t} = \frac{1}{Pr}\nabla^2 \theta, \tag{3}$$

where $\mathcal{D}$, $\boldsymbol{u}$, θ, and p represent the material derivative, the dimensionless velocity vector, temperature and pressure. Here length, time, velocity, temperature, and pressure are dimensionless with respect to D, D^2/ν, ν/D, $\Delta T = T_h - T_s$, $\rho\nu^2/D^2$. The aspect ratio of the cavity A, is defined as H/D. The properties of the liquid are the density ρ, the dynamic viscosity μ, the kinematic viscosity ν, the thermal diffusivity κ, and the thermal conductivity λ. Although deformation of the free surface is anticipated, it can be safely neglected in our model because the capillary number is sufficiently small.[7] The surface tension at the interface is considered to be a linear function of temperature: $\sigma = \sigma_s - \gamma(T - T_s)$, where T_s is taken as the saturation temperature at the vapour pressure. To complement this set of equations, an additional interfacial relation is needed.

Here we use the linearized Hertz–Knudsen equation derived from kinetic theory[3] to portray the relation between interfacial temperature and the evaporating mass flux under non-equilibrium conditions:

$$j = \alpha\rho_v L\sqrt{\frac{M}{2\pi R T_s^3}}(T_i - T_s). \tag{4}$$

It relates the local mass flux j to the local surface temperature T_i, where α is the accommodation evaporation coefficient, M is the molecular weight of vapour, R is the universal gas constant, L is the latent heat of evaporation and ρ_v is the density of the vapour.

At side walls of the cavity, we take no-slip and impermeability conditions. At the bottom porous media, only no-slip condition is enforced. The vertical velocity is derived by overall cavity mass balance. These are written as, at lateral walls,

$$u = v = 0, \quad \theta|_{x=0} = 0, \quad \theta|_{x=1} = 1, \tag{5}$$

at the bottom

$$u = 0, \quad v(x,0) = \int_0^1 v(x,A)dx, \quad \frac{\partial\theta}{\partial y} = 0 \tag{6}$$

At the interface, velocity conditions are derived from mass conservation. Selecting $\lambda\Delta T/DL$ as scale for local mass flux j and introducing a dimensionless parameter $E = \lambda\Delta T/\rho\nu L$, namely, the evaporation number,[3] which represents the ratio of the viscous to evaporative timescales, we obtain

$$v = Ej. \tag{7}$$

The surface tension plays a role in the interfacial condition, which is derived by a balance between shear stresses and thermocapillary stresses. Shear contributions from the vapour are neglected,

$$\frac{\partial u}{\partial y} + \frac{\partial v}{\partial x} = -\frac{Ma}{Pr}\frac{\partial\theta}{\partial x}, \tag{8}$$

where the parameter Ma is the Marangoni number defined as $\gamma\Delta TD/(\mu\kappa)$, and $Pr = \nu/\kappa$ is the Prandtl number. The dimensionless Hertz–Knudsen equation can be written as

$$j = Bi_{ev}\theta. \tag{9}$$

The parameter Bi_{ev}, often referred to as the evaporation Biot number,[8] is defined as

$$Bi_{ev} = \frac{\alpha D\rho_v L^2}{\lambda}\sqrt{\frac{M}{2\pi R T_s^3}}. \tag{10}$$

Equation (9) indicates that the evaporation Biot number measures the degree of non-equilibrium at the evaporating interface. $Bi_{ev} = \infty$ corresponds to the quasi-equilibrium limit, where the interfacial temperature is constant and equal to the saturation value, $\theta = 0$. $Bi_{ev} = 0$ corresponds to the non-volatile case with no evaporative mass flux.[3]

In the jump energy balance, we assume that thermal conductivity ratio and density ratio of vapour to liquid are small. The terms of viscous dissipation, kinetic energy of the leaving vapour molecules, and the

work of surface tension forces are also neglected. Then we obtain

$$Bi_{ev}\theta = -\frac{\partial\theta}{\partial y}. \tag{11}$$

From the viewpoint of heat transfer, Bi_{ev} also represents the capability of heat exchange induced by evaporation at the liquid–vapour interface.

The governing equations along with the boundary conditions are solved on a uniform staggered mesh using fully second order accurate projection method.[9] The Crank–Nicolson scheme is employed to temporally discretize the diffusive terms, and the Adams–Bashforth extrapolation is implemented for the convective terms. All the spatial derivatives are approximated by second-order central finite difference. Steady solutions are obtained when the relative variation of the primitive variables less than 10^{-8} in a marching step. The accuracy of the computing program is established by comparing solutions of high Marangoni number convection with those given by Zebib *et al.*[10]

To make our numerical investigations physically relevant, we ascertain the parameter magnitude of our model by using the properties of water with its own vapour near 4°C, at which the expansion coefficient is relatively small, exerting weak buoyancy effects.

The maximum ΔT is limited by the assumption that the temperature of the hot wall deviates little from saturation temperature, as is necessary to derive the linearized Hertz–Knudsen equation. It should also be sustained without causing nucleation. Thus $\Delta T = T_h - T_s$ is assumed to have the bound of 0.1 K to 1 K. The width of the liquid layer is assumed to fall in the range of 1 mm to 4 mm. The values of the non-dimensional numbers give $E = 10^{-4} \sim 10^{-5}$, $Ma = 10^1 \sim 10^3$, $Pr = 13.0$, $Ca = 10^{-6}$, and $Bi_{ev} = 10^2\alpha \sim 10^3\alpha$. As the accommodation evaporation coefficient α is an empirical value that can span over four orders of magnitude from 0 to 1,[11] the value of Bi_{ev} is supposed to vary from 0 to 10^3.

We introduce local mass flux $j(x, A)$ and integral mass flux $J = \int_0^1 j(x, A)dx$ to characterize the mass transfer, plus local and integral Nusselt number for the interfacial heat transfer:

$$Nu_l(x) = v(x, A)\theta(x, A) - \frac{1}{Pr}\frac{\partial\theta(x, A)}{\partial y}, \tag{12}$$

$$Nu = \int_0^1 Nu_l(x)dx. \tag{13}$$

By using Eqs. (7), (9) and (11), we obtain

$$Nu_l(x) = \Big(E\theta + \frac{1}{Pr}\Big)j(x, A). \tag{14}$$

Since the evaporation number E is on the order of $\sim O\ (10^{-5} \sim 10^{-4})$, the contribution of $E\theta$ can thus be omitted compared to $1/Pr$ in the above equation. Therefore, the local Nusselt number is regarded as $Nu_l(x) = j(x, A)/Pr$, in which the value of Nu_l is obtained when j is derived. Thus, the local Nusselt number could be represented by the local mass flux.

Our numerical simulation shows that the mass flux J and liquid temperature θ are of order unity for a wide range of Bi_{ev} value. Owing to the small value of evaporation number E, the compensation velocity in the cavity is vanishingly small according to Eq. (7). Thus the flow pattern is largely determined by the thermocapillary convection. To avoid the influence of complex flow patterns and unsteady surface tension driven flow,[12] the aspect ratio A is supposed to equal 1. We therefore mainly concern ourselves with the temperature distribution and interfacial mass and heat transfer, not the flow pattern.

The physics of the coupling of evaporation and thermocapillary convection is complicated. When investigating this problem, it is helpful to look at different aspects of the problem separately whenever possible. In this manner, we first investigate the roles that thermocapillary convection plays with demonstrating the isothermals of the cavity for different Ma at a specific Bi_{ev}, as shown in Fig. 2.

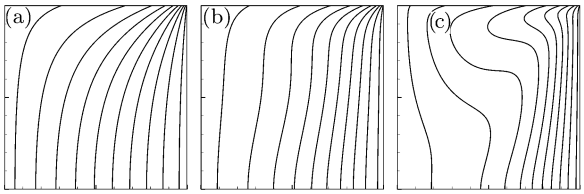

Fig. 2. Isotherms at contour intervals of 0.1 for (a) $Ma = 0$, (b) $Ma = 250$, (c) $Ma = 1000$, respectively, with $Bi_{ev} = 10$.

Thermocapillary flow carries fluid from hot region to cool region near the surface, thus elevating the temperature of the interface. The stronger the convection, the higher the temperature of the fluid at the interface. According to Eq. (9), increasing interfacial temperature conduces to larger local mass flux. In this way, thermocapillary convection has a positive influence on interfacial mass transfer.

The effect of Bi_{ev} on the temperature distribution at $Ma = 1000$ is shown in Fig. 3, which indicates that the densest isotherm region on the interface is gradually moving from the cold side to the hot side with increasing Bi_{ev}. Because Bi_{ev} represents the capability of heat exchange induced by evaporation, the elevation of Bi_{ev} leads to the decrease of the interfacial temperature, and pulls down temperature gradient at most part of the interface. This action impairs the mechanism that thermocapillary convection helps to elevate evaporating mass flux. In the last plot, the isotherms are almost entirely compressed to the hot

corner at the surface, with weak thermocapillary convection in the rest flow regions.

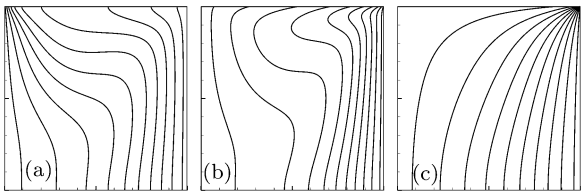

Fig. 3. Isotherms at contour intervals of 0.1 for (a) $Bi_{ev} = 0$, (b)$Bi_{ev} = 10$, (c) $Bi_{ev} = 100$, respectively, with $Ma = 1000$.

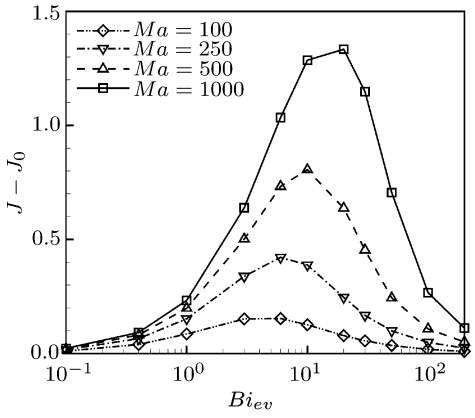

Fig. 4. $J - J_0$ versus evaporation Biot number.

To quantitatively examine the coupling of thermocapillary convection and evaporation, we consider $Ma = 100$, 250, 500 and 1000, while holding Bi_{ev} constant at 12 different values that cover four orders of magnitude. In order to show the contribution of thermocapillary convection, we employ $J - J_0$ to indicate how much mass flux is increased by this convection, where J_0 stands for the interfacial integral mass flux with no convection.

Figure 4 reflects the contribution of thermocapillary convection to mass transfer responding from steady flows at various evaporation Biot numbers. Greater evaporation mass flux is acquired with higher Marangoni numbers at all levels of Bi_{ev}. However, the contribution of thermocapillary convection largely depends on Bi_{ev}. We identify three steady-state evaporation regimes to depict the coupling mechanism. For $Bi_{ev} > 100$, in terms of the analysis of Fig. 3, thermocapillary convection is rather weak at the interface. Thus it accounts little for evaporation flux. For $Bi_{ev} < 1$, although the thermocapillary convection dominates for the heat transfer in the liquid layer, the contribution of convection to the evaporation flux is still limited, for the liquid is nearly non-volatile. Only at moderate Bi_{ev} values can thermocapillary have apparent influence on interfacial mass transfer, as shown that $J - J_0$ achieves its maximum value when Bi_{ev} is on the order of $O(10^1)$ for all these Marangoni numbers.

These three regimes are a consequence dictated by the competition between phase change and thermocapilliarity. On the one hand, thermocapillary convection carries heat from the hot wall to the cold wall, resulting in an increase of interfacial temperature compared to pure evaporation case. On the other hand, large evaporation Biot number favours high evaporation mass flux at fixed interfacial temperature. Thus, it seems that increasing Ma and Bi_{ev} acts a positive part in speedup of evaporation. However, the surface temperature in this model is not fixed, but the coupling result between convection and evaporation. Therefore, on the contrary, increasing Bi_{ev} produces two negative effects on evaporation: larger Bi_{ev} not only decreases the interfacial temperature to be more close to the saturation one, but also flats the interfacial temperature space distribution and thus impairs thermocapillary convection.

In conclusion, previous scholars only studied the influence of Marangoni convection on evaporation flux at thermodynamic equilibrium conditions. However, these models are not very effective at elucidating the effect of thermocapillary convection on evaporation flux at different non-equilibrium states. In our evaporation–thermocapillary model, the coupling mechanism of evaporation and thermocapillary convection has been expounded. Additionally, we first find three steady-state evaporation regimes depicting the evaporation mass and heat transfer under thermocapillary convection. These regimes have been successfully explained in the above discussion.

References

[1] Colinet P, Legros J C and Velarde M G 2001 *Nonlinear Dynamics of Surface-Tension-Driven Instabilities* (Berlin: Wiley-VCH)
[2] Palmer H J 1976 *J. Fluid Mech.* **75** 487
[3] Burelbach J P, Bankoff S G and Davis S H 1988 *J. Fluid Mech.* **195** 463
[4] Shih A T and Megaridis C M 1996 *Int. J. Heat Mass Transfer* **39** 247
[5] Ravino R and Fico S 2004 *Phys. Fluids* **16** 3738
[6] Hu H and Larson R G 2005 *Langmuir* **21** 3972
[7] Davis S H 1987 *Ann. Rev. Fluid Mech.* **19** 403
[8] Liu R, Liu Q S and Hu W R 2005 *Chin. Phys. Lett.* **22** 402
[9] Liu M, Ren Y X and Zhang H 2004 *J. Comput. Phys.* **200** 325
[10] Zebib A, Homsy G M and Meiburg E 1985 *Phys. Fluids* **28**(12) 3467
[11] Marek R and Straub J 2001 *Int. J. Heat Mass Transfer* **44** 39
[12] Peltier L J and Biringen S 1993 *J. Fluid Mech.* **257** 339